PERGAMON

Atmospheric Environment 33 (1999) 2549–2562

ATMOSPHERIC ENVIRONMENT

Identification of source nature and seasonal variations of Arctic aerosol by the multilinear engine

Yu-Long Xie[a], Philip K. Hopke[a,*], Pentti Paatero[b], Leonard A. Barrie[c], Shao-Meng Li[c]

[a] *Department of Chemistry, Clarkson University, Potsdam, NY 13699-5810, USA*
[b] *Department of Physics, University of Helsinki, P.O. Box 9, FIN 00014, Finland*
[c] *Atmospheric Environment Service, 4905 Dufferin Street, Downsview, Ont. M3H5T4, Canada*

Received 19 December 1997; accepted 8 May 1998

Abstract

Samples of airborne particulate matter were collected over a continuous sequence of 1 week intervals at Alert, Canada beginning in 1980 and analyzed for a number of chemical species. It was found that the measured weekly average concentrations display strong, persistent seasonal variations. In another recent study, the measured concentration of 24 constituents were arranged into both 2-way and 3-way data arrays and bilinear and trilinear models were used to fit the data using a new mathematical technique, positive matrix factorization. Five factors were found to explain the data for both 2-way and 3-way modeling with each factor representing a likely particle source. In the 2-way modeling, the yearly cyclical seasonal variations were not directly retrieved since the whole 11 yr of data was regarded as a single mode in the fitting. In the 3-way analysis, assuming the week-to-week patterns of the source contributions recur from year to year imposed fixed seasonality on the solutions. The resulting fit becomes worse if the year-to-year pattern of variation is not identical for any given source. These results suggested that a mixed model containing both 2-way and 3-way components might provide the best representation of the data. The methodology to calculate such a mixed model has just been developed. The multilinear engine is introduced in this study to estimate a mixed 2-way/3-way model for the Alert aerosol data. Five 2-way and two 3-way factors have been found to provide the best fit and interpretation of the data. Each factor represented probable source with a distinctive compositional profile and seasonal variations. The five 2-way factors are (i) winter Arctic haze dominated by SO_4^{2-} including metallic species with highest concentrations from December to April, (ii) soil represented by Si, Al, Ca, (iii) sea salt, (iv) sulfate with high acidity peaking in late March and April and (v) iodine representing most of the observed I with two maxima, one around September and October and another around March and April. The two 3-way factors are (i) bromine characterized by a maximum in the spring around March and April; and (ii) biogenic sulfur which includes sulfate and methanesulfonate with maxima in May and August. The acidic sulfate, bromine, and iodine factors have a common maximum around March/April, just after polar sunrise, suggesting the influence of increased photochemistry at that time of year. The strength of the year-to-year biogenic sulfur factor showed a moderate correlation ($r^2 = 0.5$) with the yearly average Northern Hemisphere Temperature Anomaly suggesting a relationship of temperature with biogenic sulfur production. The results obtained are consistent with those obtained in the previous study and agree with the current understanding of the Arctic aerosol.

Keywords: Arctic haze; Multiway factor analysis; Time-series analysis; Biogeochemical cycles; Multilinear engine

* Corresponding author.

1352-2310/99/$ - see front matter
PII: S1352-2310(98)00196-4

1. Introduction

During the last two decades, there has been an increasing interest in air pollution in the Arctic. Arctic haze, as it is called, is marked by a reduction of visibility, and the occurrence of elements, ionic species, and organic compounds that are found in anthropogenic emissions and in concentrations greatly in excess of those expected for a pristine environment. It has also been recognized that the Arctic aerosol consists of both man-made pollution and natural sources like wind-blown soil dust, sea salt, reaction products of gaseous marine emissions and other volatile species (Barrie, 1986). The aerosol concentration in the Arctic has a strong seasonal variation generally characterized by a summer minimum and a winter maximum. Furthermore, during the winter, the majority of the particulate matter has been attributed to anthropogenic origins while in summer, the lower concentrations are contributed mainly by natural sources (Barrie, 1986; Barrie and Hoff, 1985). It has been demonstrated that Arctic haze consists of various components that may represent several types of aerosol carried by different air masses or from different sources (Heidam, 1981). Therefore, a relatively simple physical structure for the Arctic aerosol might be assumed (Barrie and Hoff, 1985; Barrie and Barrie, 1990). In order to understand the real or potential effects of the Arctic air pollution to the polar ecosystem and global climate and to develop an appropriate strategy for controlling the extent of Arctic air pollution, the nature of the man-made pollutants, the origins of these chemical species, the mechanism and the preferred pathways for the long-range transport and the transformation of gaseous compounds in the atmosphere that occurs in the cold polar region need to be understood.

To apportion the measured aerosol concentrations to their sources, receptor models are often used (Hopke, 1988, 1991). There are two main branches of receptor models, chemical mass balance (CMB) and multivariate models. In CMB, the number and nature of the sources is assumed to be known. Multivariate receptor models are usually a form of factor analysis and are used because they can determine both the source apportionment and composition of the sources without a priori knowledge of the sources and their composition. The data matrix for factor analysis is obtained by measuring various chemical species and/or physical properties for a sequence of samples. Principal component analysis (PCA) (Barrie and Barrie, 1990) has often been applied to the data matrix. The principal components explaining the majority of variance of the data matrix are interpreted as possible sources as identified from the factor loadings of the measured species, generally after a rotation of factor axes.

Heidam (1981) first applied principal component analysis for the source identification of Arctic aerosol. Barrie and Barrie (1990) identified four sources including soil, sea salt, anthropogenic aerosol and a fourth factor associated with photochemical reaction. Because of substantial numbers of missing data and values below detection limit in the measurements, especially during the summer period, only winter data were used in the principal components analysis. The inability to treat the missing data that are a common occurrence in environmental investigations is a problem for the widely used PCA and related techniques. They also suffer from a more fundamental limitation (Paatero and Tapper, 1993) in that the PCA analysis in effect weights the data points in an inappropriate manner. The results of PCA cannot provide a true minimum variance solution since they are based on an incorrect weighting (Paatero and Tapper, 1993). Finally, the factors of PCA are rarely physically explainable without rotation, and no fully satisfactory rotation has yet been found (Henry, 1987). Although identification of four possible sources was obtained by inspecting the relative magnitude of principal component loadings, the corresponding scores do not provide a quantitative apportionment. Thus, seasonal variations of the possible sources were examined by studying the time series of four specific chemical species each chosen to represent a different source obtained by the PCA (Barrie and Barrie, 1990).

Given PCA's limitations, a new mathematical technique, positive matrix factorization (PMF), was developed by Paatero and Tapper (1994) to address problems associated with the standard PCA. This new technique gives weights to the individual data points based on the error estimates for the individual measurements. Non-negatively of the resulting factors is also integrated in the computational process. These are very useful features for the receptor modeling of environmental data because error estimates are usually available in the air pollution monitoring data, and the source compositions and contributions must be non-negative. In addition, missing or below detection limit data can be included in the analysis by assigning appropriate values with large error estimates. This feature enables the information in the data set to be incorporated as completely as possible into the analysis.

In a previous study, PMF was successfully applied to data from Alert (Xie et al., 1998). In order to explore the nature of the cyclical variation of the different processes that give rise to the measured concentrations, the observations were arranged into both a 2-way matrix and a 3-way data array. To address the periodicity within each year, the three modes were defined as the chemical constituents, the week within a year, and the year within the 11 yr data record. Thus, seasonal variations, long-term trends and source profiles of each probable aerosol source could be obtained in the 3-way analysis. Five factors were derived from both *pure* 2-way and *pure* 3-way PMF analyses and quantitative compositional

profiles and distinctive seasonal variations in the source contributions were obtained. Even though both *pure* 2-way and *pure* 3-way analyses showed consistent results, important differences still exist. In 2-way modeling, the whole 11 yr data was regarded as a single mode in the fitting, so yearly cyclical seasonal variations were not assumed and thus not directly recovered by the analysis. In the 3-way analysis, the week-to-week pattern of the source contributions was forced to recur identically from year to year. The fit for the 3-way analysis became worse because the year-to-year variations were not identical for all of the sources. These results suggest that both bilinear and trilinear models may reflect only part of the variability of the data, and a combination of both 2-way and 3-way models might be more suitable to describe the Alert data.

Very recently, Paatero (1998) invented a new mathematical tool called the multilinear engine for solving the general multilinear problem. In ME, any kind of multilinear modeling problem is represented by a set of equations, each of which approximates one data value, by a sum of products of unknowns (factor elements). Different unknowns are defined for different data values according to the prescribed model structure. Therefore, the ME model is very flexible and provides a general framework for different multilinear models including *pure* bilinear and trilinear models as well as a mixed 2-way/3-way model as will be used in this study. It is worthwhile to note that ME retains all of the main features of PMF including weights for individual measurements based on measurement uncertainties and non-negativity constraints that are important in many environmental applications.

In this investigation, a mixed 2-way/3-way model has been assumed for the modeling of the complete set of aerosol measurements from Alert, N.W.T., Canada between September of 1980 and August of 1991 and ME was applied to solve the problem. In the next sections, the data will be described, the ME approach briefly introduced, and the results of the analysis presented and discussed.

2. Sampling, analysis, and data pretreatment

Aerosol samples have been collected at Alert, Northwest Territories, Canada (latitude 82.3 N, longitude 62.5 W) by the Atmospheric Environment Services (AES) of Canada on a weekly basis since July 1980. Details of the sampling and procedures of chemical analyses were given by Barrie and Hoff (1985) and Barrie et al. (1989). Major ions were analyzed by ion chromatography (IC) and trace elements data were obtained by instrumental neutron activation analysis (INAA) and by inductively coupled plasma emission spectroscopy (ICP). Some species have measurements from different analytical techniques. The consistency of the data from different analytical techniques has been checked and no significant differences were observed, so the data from the analytical technique having the most complete measurements and best detection limits were retained for the data analysis. Detection limits (DL) were available for part of the INAA data, but no detection limits were directly available for the IC and ICP measurements. The range of average detection limits for the different analytical techniques were given by Barrie and Hoff (1985) and Barrie and Barrie (1990). Based on their table and the available detection limits associated with the data files, average detection limits for each chemical species were estimated for use in this application.

A detailed summary of statistics of the chemical concentrations of aerosol species has been reported and a comprehensive frequency distribution analysis suggested that most of the species are lognormally distributed (Cheng et al., 1991). Some elements like the rare earths have very low concentrations and covary with other elements. Their measurements were only made for a limited time period and preliminary data analysis results that included them showed them to have little significance on the results. Thus, they were excluded in the current study. The final data set included 24 chemical species measured in the samples obtained between September 1980 and August 1991. The species have up to 532 weekly average concentrations and not all of the species have the same number of data values. Average concentrations (geometric mean) were assigned to the missing data and their influence on the fitting was constrained by giving relative large error estimates (Lower weights). Three-way modeling requires the 2-way data matrix to be arranged into a 3-way data array with the same number of weekly samples (approximately 52 weeks) in each year. In order to make each year have the same number of weeks for the whole 11 yr, 40 extra entries were added in the appropriate time positions for all the species and their values were assigned as the corresponding geometric mean. Thus, there are at least 40 missing data points for each species. Table 1 lists the 24 elements used together with the features of their measurements. In the organization of the data array, an attempt has been made to synchronize the data from year to year. A 572 by 24 data table has been created which was viewed as a 52 by 11 by 24 3-way data array when 3-way modeling was performed.

3. Data analysis

3.1. Nomenclature

Bold lower case letters are used for vectors and bold upper case letters for matrix and 3-way data array. The

Table 1
The analytical method, geometric mean and estimated average detection limit of measured concentration for each aerosol constituent

Aerosol constituent	Analytical method	Geometric mean (ng m^{-3})	Detection limit (ng m^{-3})	No. of missing values	No. of values below DL[a]	No. of available DL[a]
Cl^-	INAA[b]	63	2.5	47	71	356
Br^-	INAA[b]	2.6	0.35	52	103	358
NO_3^-	IC[c]	45	1.5	40	0	0
SO_4^{2-}	IC[c]	490	4	40	0	0
H^+	IC[c]	1	0.3	44	201	0
Na^+	INAA[b]	100	4	52	23	356
NH_4^+	IC[c]	57	6	40	12	0
K^+	IC[c]	7.3	3	43	147	0
MSA	IC[c]	4.3	2	40	120	0
Mn	INAA[b]	0.75	0.15	52	63	356
V	INAA[b]	0.28	0.05	52	86	356
Al	INAA[b]	65	1.5	52	1	356
Zn	ICP[d]	2.3	1	60	122	0
Pb	ICP[d]	0.6	0.2	46	91	0
Ca	INAA[b]	70	10	52	12	356
Ti	INAA[b]	5	6	52	369	356
I^-	INAA[b]	0.24	0.015	52	37	358
In	INAA[b]	0.0007	0.0003	52	221	358
Si	INAA[b]	190	65	108	85	301
As	INAA[b]	0.13	0.05	52	19	355
La	INAA[b]	0.03	0.02	52	184	355
Sb	INAA[b]	0.025	0.06	52	52	355
Sm	INAA[b]	0.008	0.0005	52	8	327
Sc	INAA[b]	0.02	0.015	51	193	364

[a] Detection limit.
[b] Instrumental neutron activation analysis.
[c] Ion chromatography.
[d] Inductively coupled plasma – atomic emission.

same letters in plain stand for scalars if associated with subscripts. In the latter situation, letters with subscript indices are the elements of the corresponding vector, matrix, or 3-way data array that letters stand for. Other plain letters are used for scalars as well.

3.2. The multilinear engine

The multilinear engine (ME) (Paatero, 1998) is a new concept for solving a variety of multilinear problems. The multilinear model can be written in the sums-of-products form

$$x_i = y_i + e_i = \sum_{k=1}^{K_i} \prod_{j \in \zeta_{ik}} f_j + e_i \quad (i = 1, \ldots, M), \tag{1}$$

where the index i enumerates the equations which form the model to be solved. Essentially each equation corresponds to each of the measured value x_i. Auxiliary equations can be used to represent any a priori information and/or some constraints such as smoothing, rotation, etc. needed for the solution. M denotes the number of the equations, which is the sum of the number of the measured values and the number of auxiliary equations, if any. The fitted value y_i for each data point x_i is represented as a sum of product of all factor elements $f_j (j \in \zeta_{ik})$. K_i indicates the number of product terms in each equation. For equations corresponding to a *pure* 2-way PCA or a *pure* 3-way trilinear model, the values K_i equal to the number of factors. The elements j of the index sets ζ_{ik} are the indices of those factor elements, f_j, that form the kth product term of the ith equation. Finally, e_i is the unmodeled part of data x_i.

Determining the best fit according to Eq. (1) is equivalent to solving the following minimization problem:

$$\min_f Q(x, f), \tag{2a}$$

where

$$Q(x, f) = \sum_{i-1}^{M} \left(\frac{e_i}{\sigma_i}\right)^2 = \sum_{i=1}^{M} \left(\frac{x_i - \sum_{k=1}^{k_i} \prod_{j \in \zeta_{ik}} f_j}{\sigma_i}\right)^2$$

$$f_j \geqslant 0 \quad (j \in 1, \ldots, N) \tag{2b}$$

and the values σ_i are the uncertainties connected with the measurements; typically σ_i is the standard deviation of the measured value x_i, N is the number of the elements of all the factors.

The formulation of the system of equations in Eq. (1) is extremely general. To facilitate the understanding of the principle of ME, a system of equations representing a mixed 2-way/3-way model is provided as a more practical example:

$$X_{ijk} = \sum_{q=1}^{Q} T_{ikq} G_{jq} + \sum_{p=1}^{P} A_{ip} B_{jp} C_{kp} + E_{ijk} \times \begin{pmatrix} i = 1, \ldots, I \\ j = 1, \ldots, J \\ k = 1, \ldots, K \\ p = 1, \ldots, P \\ q = 1, \ldots, Q \end{pmatrix}. \quad (3)$$

The first term represents a customary Q factor 2-way PCA model with score and loading matrices **T** and **G**, while the second term is a P factor 3-way trilinear model with the **A**, **B**, and **C** matrices being the three modes, respectively. For the Alert data, factor **T** contains time variation over the entire 11 yr, and **G** provides concentration profiles of the corresponding sources from 2-way modeling. Factor matrices **A** and **C** correspond to the time variation during a year and across 11 yr, respectively, and **B** is the source concentration profile matrix in the 3-way part of the model. In Eq. (3), X_{ijk} and E_{ijk} have the same meaning as x_i and e_i as in Eq. (1). In ME programming, a mapping must be specified from 2-way or 3-way array **X** to a long vector **x**, and from all of the 2-way and 3-way factor matrices **T**, **G**, **A**, **B**, **C** to a long factor vector of unknowns, **f**. The entire mapping is done by pre-processing and post-processing programs. The summation of the first two terms makes the fitted part of data, y_i, in Eq. (1). The index subset ζ_{ik} in Eq. (1) denotes the indices of corresponding elements of **T**, **G**, **A**, **B** and **C** factors in the long vector **f** for a specific data point. Therefore, in the ME model, there are only the elements of the long factor vector **f** and no distinction is made between 2-way and 3-way factors.

Since there is a 3-way portion of the model, the data itself must be presented in the form of a 3-way data array as well. For the same reason, the logically two-dimensional factor matrix **T** is represented with three indices. Considering the $I \times K$ slice $\mathbf{X}_{\cdot j \cdot}$ of **X** that are obtained by fixing the second index j. These **X** slices are approximated by the linear superposition of two different entities: (i) the $I \times K$ slices $\mathbf{T}_{\cdot\cdot q}$ and (ii) the outer product slices $\mathbf{A}_{\cdot p}\mathbf{C}_{\cdot p}$. The coefficients for the superposition are contained in the factor matrices **G** and **B**, which would have a similar interpretation in terms of the physical system being modeled.

3.3. Data arrangement

Like PMF, successful application of ME requires suitable error estimates reflecting the quality and reliability of each individual measurement. Since a comprehensive frequency distribution analysis suggested that most of the species are lognormally distributed (Cheng et al., 1991), a lognormal error model was used in the ME analysis. This lognormal error model was used in the ME analysis to allow iterative re-weighting of the data points to reduce the influence of extreme values. The logarithms of the geometric standard deviation (log (GSD)) for each measured value must be specified in order to solve the factorization with the lognormal error model. Empirically, the same value is adequate to present the variability of all the measured points for each species, so a constant could be used as the estimate. As in the PMF analysis (Xie et al., 1998), a modification for the *pure* lognormality was adapted by superimposing an additional normally distributed error onto the lognormal distribution. The detection limits were used as such an additional additive term in the error matrix elements in order to avoid zero values, which would make the factorization unstable. In this investigation, a constant of 0.3 was used as an estimate of the log (GSD) for all the data points, and the measured detection limits were used as the additional additive terms. Since not all of the data points had directly determined detection limit values, estimates of detection limit were made for those data points. Based on the published detection limit range by Barrie et al. (Barrie and Hoff, 1985; Barrie and Barrie, 1990) and the detection limits that were partially available for the data, average detection limits for each species were estimated and are listed in Table 1. In our experience to date, it appears that fully accurate estimates of detection limits are probably unnecessary.

There are some negative values in the data set resulting from the subtraction of blank values. These values were treated as if they were values below detection limits and were replaced by half of the corresponding average detection limits listed in Table 1. Missing data were replaced by the corresponding geometric means tabulated in Table 1. For below detection limit values, the error was assigned as the average detection limit while for the missing values, the errors were set to be twice the geometric mean. A few abnormal data points for Ti (3), I (1), Sm (1) and Zn (2) were also identified by inspecting the species-pair scatter plots. It appears that they may be decimal point errors and appropriate changes in the decimal point positions were made.

3.4. Normalization of the resulting factors

The data analysis will provide factors associated with concentration profiles and time variations. Since the total airborne particle mass concentrations were not

measured, it is not possible to obtain absolute concentration profiles from the data analysis. However, the time factor(s) should be dimensionless. If we normalize the time factors to a unit mean, and then multiply the normalization coefficient into the concentration profile factors, the outer product will maintain the units of the measured concentrations. Such normalization produces concentration profile factors with the measured concentration unit. Therefore, the following normalization were used in the ME program for the mixed 2-way/3-way model used in this study:

$$\begin{cases} A_{ip} = \dfrac{A_{ip}}{n_{Ap}}, & n_{Ap} = \dfrac{\sum_{i=1}^{I} A_{ip}}{I} \\ C_{kp} = \dfrac{C_{kp}}{n_{Cp}}, & n_{Cp} = \dfrac{\sum_{k=1}^{K} C_{kp}}{K}, \\ T_{ikq} = \dfrac{T_{ikq}}{n_{Tq}}, & n_{Tq} = \dfrac{\sum_{l=1}^{I\times K} T_{lp}}{I\times K}, \end{cases}$$

$$\begin{cases} B_{jp} = \dfrac{B_{ip}}{n_{(B+G)j}} \\ G_{jq} = \dfrac{G_{jq}}{n_{(B+G)j}} \end{cases} \quad n_{(B+G)j} = \sum_{p=1}^{P} B_{jp} + \sum_{q=1}^{Q} G_{jq}. \tag{4}$$

From the direct ME output of **B** and **G** factors, one can see how a species distributed in different **B** and **G** factors, i.e. the relative importance of a species in different sources. To get the source profiles with "absolute" concentration unit, the **B** and **G** factors need to be renormalized in the following way:

$$\begin{cases} B_{jp} = B_{jp} \times n_{Ap} \times n_{Cp} \times n_{(B+G)j} \\ G_{jq} = G_{jq} \times n_{Tq} \times n_{(B+G)j} \end{cases} \tag{5}$$

4. Results and discussion

First, the dimensionality of the fitted model needs to be determined. Unlike PCA, the results of the ME analyses are not hierarchical, i.e. a higher dimension solution does not contain all the factors of the lower dimensions, because orthogonality is not required. All of the factors may change when the dimension is varied. Therefore, ME modeling was performed with different combinations of 2-way/3-way factors, i.e. different mixed models. Since random numbers were used as initial estimates of factor elements and the conjugate gradient curve fitting algorithm was used in the ME minimization, there is no guarantee that a single ME run will find the global optimum. Therefore, six repetitions were made for each mixed model. The results were then inspected and compared. The mixed models that were examined included four 2-way and two 3-way model (abbreviated as $4+2$), $4+3$, $5+2$, $5+3$, and $5+5$ models. Even though different factor solutions were obtained for different mixed models and several local optima were found for a given model, some of the results were stable and they occur similarly in all the solutions. It appeared that five 2-way and two 3-way ($5+2$) mixed model provided the best fit of the model to the data and the resulting factors were most interpretable. Generally, insignificant factors were obtained if more factors were used and much worse fits were obtained when fewer factors were used.

The factors provided by the ME were physically interpretable, but rotational ambiguity still exists. Some factors included species that obviously should not exist in such factors. Compared to PCA, the rotational ambiguity was considerably reduced by applying natural constraints such as factor non-negativity. However, the commonly used natural physical constraints are insufficient to guarantee a unique, physically valid solution as indicated by Henry (Henry, 1987). In this application, rotation was applied. The solution offering the best fit in the six repetitions of ($5+2$)-mixed model was chosen as the basis of rotation. Since the unrotated factors were already quite physically reasonable and only one or two factors were contaminated by species that obviously should not be present, rotation was rather simple. The rotations were made in such a way so as to reduce the amplitude of the inappropriate species in the factors in question and the acceptable rotations were examined by trial and error. Although human intervention brings a degree of subjectivity to the results, there were good reasons that permitted experience and other results in the analysis.

The solution of $5+2$ mixed model after rotation is presented. The optimization criteria, Q values defined in Eq. (2), are 12 061 for unrotated solution and 12 422 after rotation. The trivial difference in the Q values before and after rotation suggested that the rotation did not add a penalty, which means that the data structure was maintained after rotation and only the axes for representing the data were changed. Since the Q values approach the theoretical Q, which is the number of data points (13 728), the model fits the data well. The fit obtained with this mixed mode model was better than either the pure 2-way and 3-way PMF models.

Figs. 1 and 2 present the five 2-way factors of the mixed model. The left side of Fig. 1 shows the factors associated with chemical composition which are the **G** factors outputted directly from ME program. Since the summation of the magnitude of each species across all the five 2-way **G** factors and two 3-way **B** factors (see Fig. 3) is unity, the magnitude of a species in a factor reveals the percentage contribution to the species from the source represented by the factor. Displayed on the right side are the **G** factors after renormalized based on Eq. (5) so that they provide the chemical composition of each factor. They are the relative compositional profiles of the identified sources.

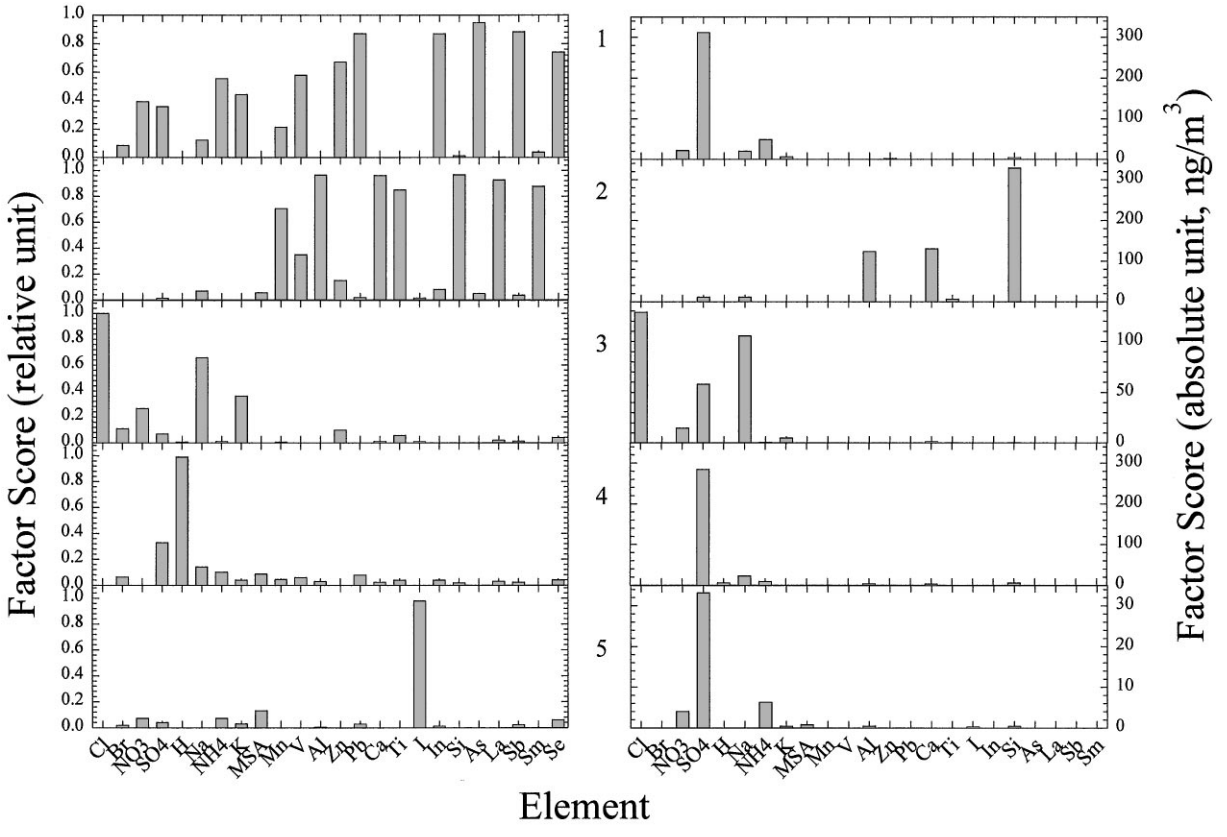

Fig. 1. **G** factors of 2-way modeling, *left*: relative contribution of species to factors; *right*: absolute composition of each factor (source profiles).

The five factors presenting the temporal variation are shown on the left side of Fig. 2. In order to facilitate the investigation of the assumed yearly cyclical seasonal variation of each possible source and to compare with the counterpart 3-way modeling, the 11-yr temporal variation factors were folded into 11 separate year-long sections and displayed as overlapping curves in the right part of Fig. 2.

Figs. 3–5 presents the 3-way factors of the mixed model. The left side of Fig. 3 shows the **B** factors directly from ME program and on the right side are the **B** factors after renormalization, i.e. the source profiles. Two mode factors, **A** and **C**, referring to time variations in the 3-way analysis are shown in Figs. 4 and 5, respectively. Fig. 4 presents the seasonal variation within a year and Fig. 5 shows the year-to-year trends over the 11-yr period. Based on the source profiles shown in Figs. 1 and 3, the primary constituents of each of the possible sources are summarized in Table 2.

In order to check the fitness of the modeling, the weighed residuals of the model, the residuals divided by the standard deviations of the data points, were calculated for each species. Fig. 6 shows the frequency distribution of the weighed residuals for the major species. It can be seen from Fig. 6 that the weighed residuals of most species are within the range of ± 3 + units. Thus, one can conclude that quite good fits to the data have been achieved.

It can be seen in Fig. 1 that the first 2-way factor contains more than 30% SO_4^-, about 40% NO_3^-, high percentage of NH_4^+, K^+ and the majority of V, Zn, Pb, In, As, Sb and Se which are considered to be of anthropogenic origin. Sulfates comprise approximately 30% of the total mass of suspended particulate matter in the Arctic atmosphere (Barrie, 1986; Barrie and Barrie, 1990). The winter sulfate is the result of fossil fuel combustion and processing of sulfide ores that release SO_2 which is subsequently converted to secondary sulfate. The oxidation rate and residence time of sulfur dioxide in the Arctic atmosphere has been studied (Barrie and Hoff, 1984). Investigation also apportioned sulfate into a variety of sources, which showed that about 62–74% of sulfate in the summer and 78–85% of sulfate in the winter are of anthropogenic origins (Li and Barrie, 1993; Li et al.,

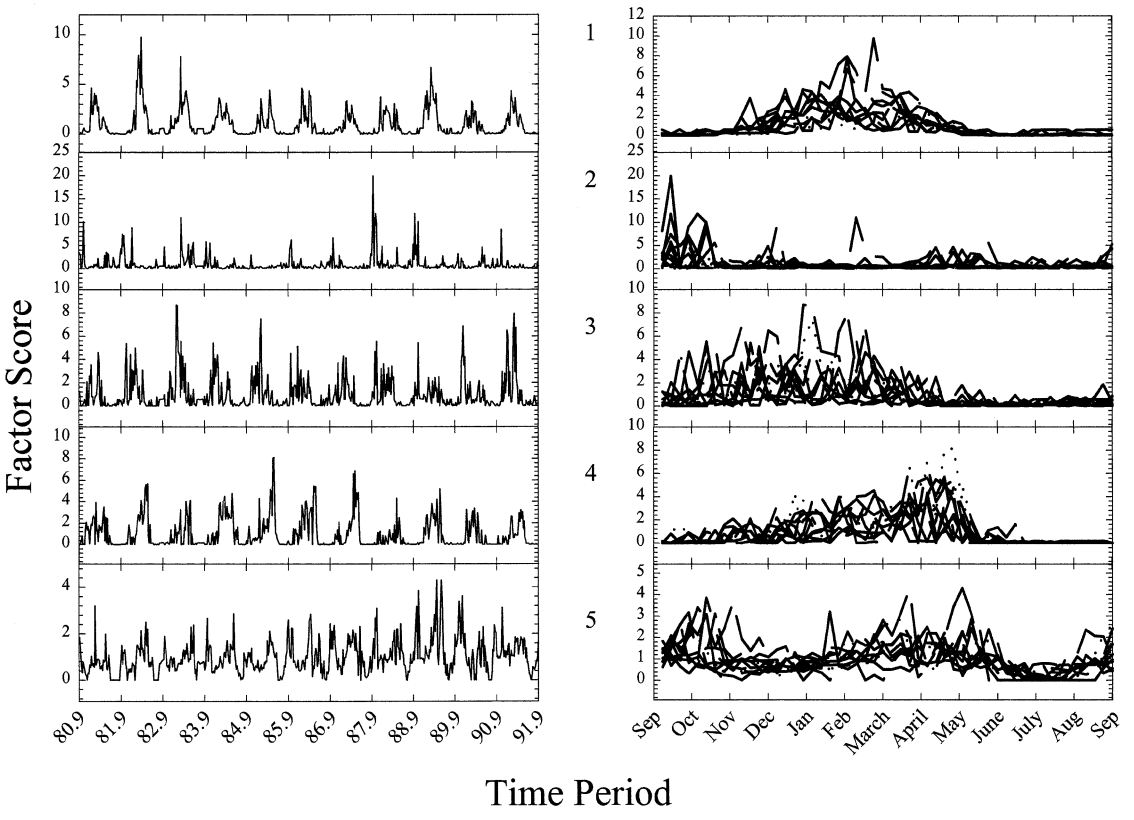

Fig. 2. **F** factors of 2-way modeling, *left*: time series of the whole 11 yr; *right*: A year-by-year overlapping representation of the **F** (time series) factors.

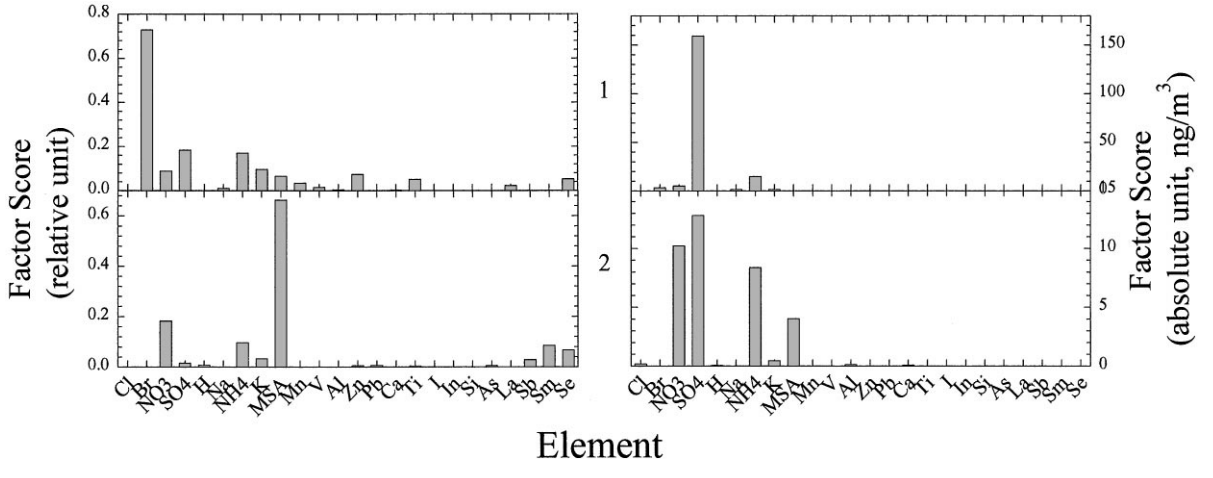

Fig. 3. **B** factors of 3-way modeling, *left*: relative contribution of species to factors; *right*: absolute composition of each factor (source profiles).

1993). The results of an analysis of the isotopic composition of sulfur in the Arctic haze suggested that most of the sulfur comes from Europe rather than more local area (Nriagu et al., 1991).

With the aide of meteorological information, Cheng et al. (1993) and Hopke et al. (1995) investigated the source locations and preferred pathways for sulfur transported to Alert by using the potential source contribution

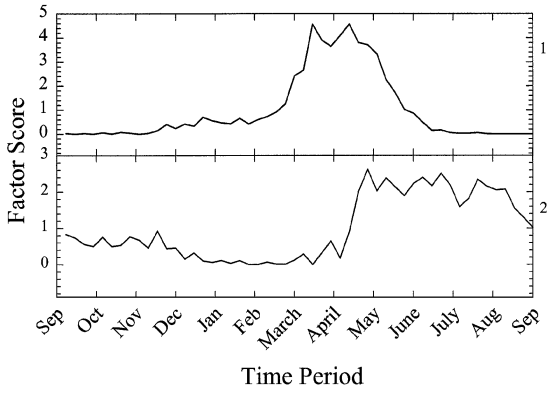

Fig. 4. **A** factors of 3-way modeling (seasonal variation).

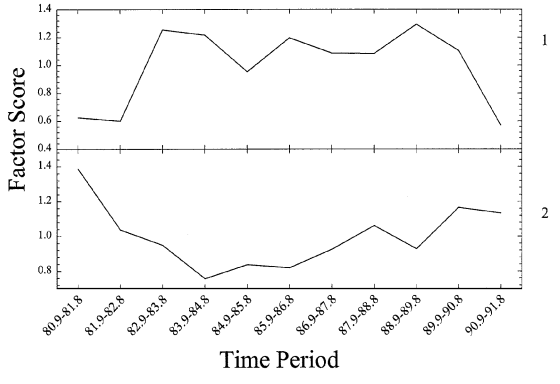

Fig. 5. **C** factors of 3-way modeling (time trend).

function (PSCF). In winter, anthropogenic SO_4^- has high PSCF patterns in Europe, eastern Canada or off the East Coast of North America which coincides with the known emissions in these areas. The high PSCF areas in central Canada and near the Urals in Russia are close to the locations of known smelting activities. No high PSCF patterns were found in summer which reflects the fact that there is very poor transport of material into the Arctic region and the strong removal of particulate SO_4^- by precipitation during the summer.

Besides the major constituent sulfate, the other species K^+, V, Zn, Pb, In, As, Sb and Se are generally considered to be associated with anthropogenic activities. NH_4^+ is generally associated with SO_4^- that has had the time to react with gaseous NH_3 (Barrie and Barrie, 1990). K^+ can be partially attributed to combustion of biomass. Pb comes mainly from antiknock agents in gasoline and from non-ferrous metal smelting. Zn can be emitted from

Table 2
The composition of each of the factors identified in the 5 + 2 ME analysis

Factor	Constituents	Possible source origin
1	SO_4^{2-}, NO_3^-, NH_4^+, K^+, Mn(?), V, Zn, Pb, In, As, Sb, Se	Anthropogenic
2	Mn, V(?), Al, Ca, Ti, Si, La, Sm	Soil
3	Cl^-, Na^+, SO_4^{2-}, K^+	Sea salt
4	H^+, SO_4^{2-}	Acidic photochemical
5	I^-, SO_4^{2-}, NO_3^-	Iodine, (acidic photochemical)
6	Br^-, SO_4^{2-}, NO_3^-, NH_4^+,	Bromine, (acidic photochemical)
7	MSA, SO_4^{2-}, NO_3^-, NH_4^+	Biogenic sulfur

non-ferrous metal production process such as copper–nickel production or municipal solid waste incineration. The elements, Sb, As are most probably released from fossil fuel combustion and Sb also seems to be associated with incinerators. In is an indicator of smelting and Se probably comes from coal burning, while V comes from fuel oil combustion. It can be seen from Fig. 2 that this anthropogenic factor has a concentration maximum starting from December and extending to February, i.e. winter Arctic haze.

The PSCF analyses were also done for the metallic elements (Cheng et al., 1993). The PSCF analysis suggested that high values of Pb appearing in most part of Eastern Europe, Russia, and the Baltic states, also high potential source areas were observed in the northeastern United States and Quebec in Canada. High potential areas of Zn were identified as in Siberia close to the Bering Sea; in the Alaska area; in northeastern Canada and in the vicinity of Moscow. High PSCF patterns were observed for As in central and eastern Russia and central Canada and for V in western Iberian Peninsula; the area of western Europe; the Kuznetsk area in central former USSR and two areas around Alaska.

The second 2-way factor is the source of most of the crustal elements (Mn, Al, Ca, Ti, Si, La and Sm) (left side of Fig. 1) and the concentrations in this factor is dominated by Al, Ca and Si (right side of Fig. 1). These elements are the major constituents of soil. Hence, this factor can be attributed to wind blown soil. Fig. 2 shown that the seasonal variation of soil factors featured two peaks, one around April/May and another in the late summer and early fall period from September to October.

There is a sharp peak in February of 1983 appearing in the seasonal variation of soil factor (note the single peak

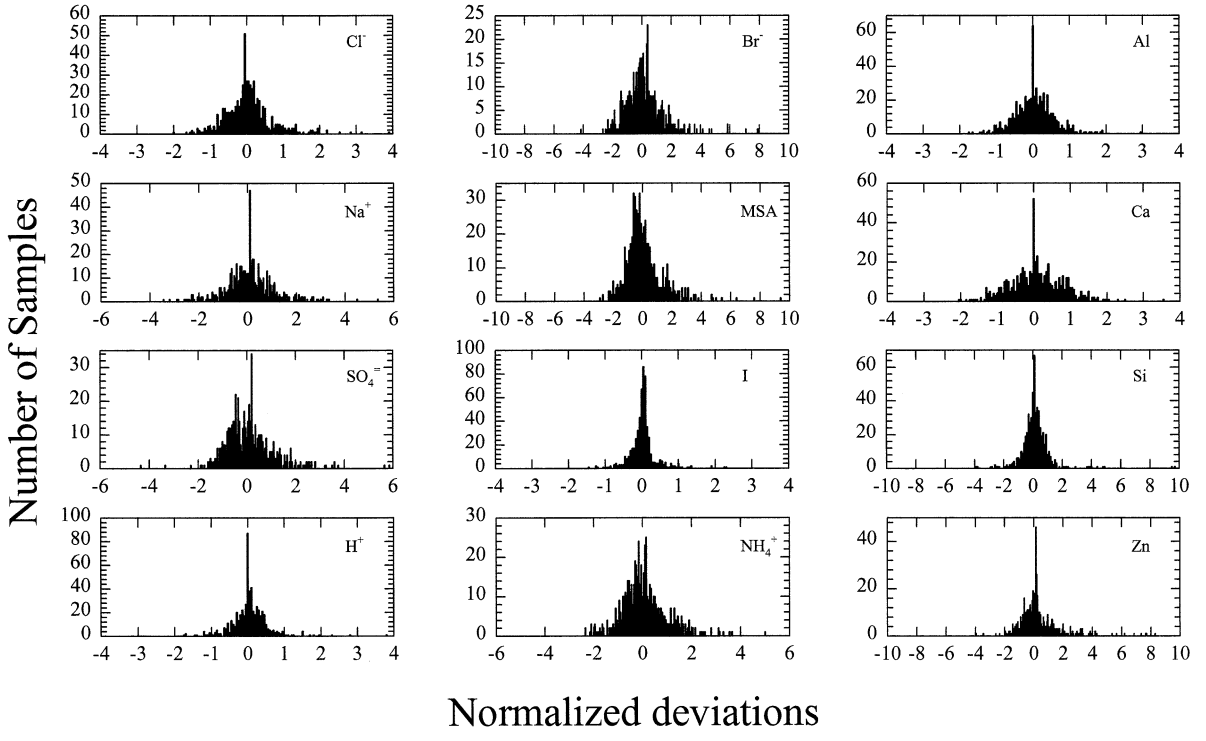

Fig. 6. Standardized residuals of some selected species from ME modeling.

in the second line on the right side of Fig. 2). By inspecting the time series of the original observations of Al, Ca, La, Sm, Mn (no Si data available for 1983), the same sharp peak was found to be present as observed in the seasonal variation of this factor. By referring to the local meteorological records, it was concluded that this peak was probably caused by blizzard weather conditions at that time.

From Fig. 1, the third 2-way factor contains most of the Cl^-, a major portion of Na^+ together with part of NO_3^-, SO_4^- and K^+, which suggests sea salt as this source of Arctic aerosol. It has a broader peak over the whole winter period from October to April. According to Barrie and Barrie (1990), this seasonal feature probably reflects stronger winds leading to longer aerosol residence times and more sea spray in the winter than in the summer.

Shown in Figs. 1 and 3, the fourth 2-way factor mainly contributes H^+ and SO_4^-. The fifth 2-way factor contains almost all of iodine, and the first 3-way factor includes mainly Br^- and SO_4^-. A common feature can be found in the seasonal variation of these acidic, iodine and bromine factors, i.e. a maximum dramatically appears in March and April just after polar sunrise. In the Arctic atmosphere, the air is at subzero temperatures in the dark during the winter and is suddenly exposed to sunlight at polar sunrise in the early spring. When the sun rises after the winter darkness, photochemical reactions occur in the atmosphere that lead to production of Br^- leading to troposphere O_3 depletion and H_2SO_4 formation from the oxidation of SO_2 (Barrie et al., 1988, 1989). A weak but significant correlation of daily I and Br concentrations was observed in spring 1988 (Bottenheim et al., 1990) and suggests common origins of iodine and bromine during the spring sunrise period. Thus, these factors represent photochemical activity factors that represents the conversion of SO_2 to acidic sulfate and the production of particulate bromine and iodine from the reaction of photochemical oxidants with sea salt (Vogt et al., 1996; Sander et al., 1997). There is a difference between bromine and iodine behavior in that there is a second peak in the late summer/early fall in the iodine factor. Barrie and Barrie (1990) also obtained a photochemical factor in their principal component analysis. The fact that a strongly negative correlation exists between filterable bromine and ozone concentration were derived from field experiments in the Arctic spring have led to extensive investigations of the mechanisms for halogen photochemistry and ozone destruction in the Arctic spring (Barrie et al., 1988; Finlayson-Pitts

et al., 1990; Bras and Platt, 1995; Vogt et al., 1996; Sander et al., 1997). The spring maximum of iodine factor suggests a photochemical production mechanism similar to that of bromine. The September iodine peak may be the result of photolysis of biogenic iodine emissions to the atmosphere during the secondary blooms in northern oceans in late summer (Barrie et al., 1990). NO_3^- may be a by-product of the oxidation of the biogenic marine gases although the link between Br^- and NO_3^- is still unclear.

The second 3-way factor is characterized by the presence of methanesulfonate (MSA) and represents a biogenic component of the Arctic aerosol. MSA is the product of the oxidation of sulfur-containing compounds like dimethylsulfide (DMS) or dimethyldisulfide (DMDS) emitted by biogenic activity in the surface layer of the ocean. Even though MSA does not contribute significantly to the total mass of Arctic aerosols, it is useful as a tracer for non-sea salt SO_4^{2-} of natural origin. From Fig. 4, it can be seen that there are two peaks in the seasonal variation of the factor, one around April/May and another about July/August. In a recent study, Li et al. (1993) postulated that the spring peak is caused by transport from oceanic sources in the North Atlantic and North Pacific and possibly by accelerated DMS oxidation in the northern atmosphere as spring solar irradiation increases in intensity. Levasseur et al. (1994) suggested that the DMS released by ice algae during ice breakup might also contribute to this peak. The summer peak was hypothesized to be due to DMS from more local/regional Arctic sources and possibly from higher-latitude northern oceans (Li et al., 1993). Ferek et al. (1995) postulated the role of more locally emitted DMS in the production of atmospheric aerosols in the Arctic in summer and their results suggested that the Arctic Ocean is potentially a substantial source of DMS, which likely becomes important as sea ice recede in the summur. Hopke et al. (1995) provided results that support these source locations.

Charlson et al. (1987) hypothesized that in order for the biogenic sulfur and could albedo feedback to exist, there must be a correlation between sea surface temperature (SST) and cloud condensation nuclei production. A necessary but not sufficient condition implied by this requirement is that there exists a correlation between SST and biogenic sulfur emissions to the atmosphere Li et al. (1993) found that correlations of monthly anomalies of MSA with those in sea surface temperature anomaly (SSTA) of the northern oceanic regions are significant for Atlantic Ocean sources in spring. Li et al. (1993) attributed the spring peak to the sea surface temperature anomalies (SSTA) in the north Atlantic ocean west of the coast of continental Europe, and the summer peak to the SSTA in ocean region further north in the Atlantic Ocean off the coast of Norway and in the northwestern north Pacific Ocean.

5. Discussion

Compared to our previous results from *pure* 2-way or 3-way PMF modeling, better resolution was obtained from ME modeling. As shown in Figs. 1 and 3 most of the species have unique attributions, like Al, Ca, Ti, Si, La, Sm in the soil factor, Pb, In, As, Sb, Se in the anthropogenic factor, Cl in sea salt, I^- in the iodine factor, H^+ in the acidity factor, Br^- in the bromine factor and MSA in the biogenic factor.

However, some species are spread over more than one factor. Two possibilities may exist. One is because of the multi-source and/or multi-mechanism of production feature of some species and thus it is reasonable for some species spreading into different factors. For example elements like Mn and V are split mainly between anthropogenic and soil factors. These multiple factors reflect the dual source nature of these elements. However, the amplitude of these elements shown in Fig. 1 is consistent with Mn being more heavily loaded on the soil factor and V on the anthropogenic one. Potassium falls mostly into the sea salt factor and the anthropogenic factor, which agrees with the observation of Barrie and Barrie (1990). Sources of atmospheric sulfur include the anthropogenic sources of fossil fuel combustion and sulfide or smelting, marine and terrestrial biogenic reduction of inorganic compounds to organic gases such as dimethyl sulfide (DMS), sea spray, volcanoes etc. Therefore, there are multiple sources expected for sulfur and thus, anthropogenic, sea salt, and biogenic sulfate in the ME analysis are quite reasonable.

During transport from the source areas to Alert, both sulfur dioxide and sulfate converted from SO_2 are present. In the dark period, there is more SO_2 than SO_4^{2-}. As the sun moves northward in the spring, more of the SO_2 is converted to SO_4^{2-} and the observed mole ratio of SO_4^{2-} to SO_2 increases from less than one in the winter time to much larger than one in the spring (Barrie and Hoff, 1984). Since the conversion occurs closer to Alert, there is less opportunity to react with NH_3 and become neutralized. Thus, the photochemical SO_4^{2-} peak is not so much representative of different sources but of a different extent of the atmospheric oxidative processes in transit.

Another possibility is because of the limits to the resolution of the data analysis. For example, small amounts of elements such as Zn, Ti, Se, etc. appear in the sea salt factor, Zn, Ti, and Se in the bromine factor and trace amount of Sb, Sm, and Se in the biogenic factor that does not appear to reflect the reality of the source emissions but may be the result of the general similarity in the annual time variations of these species because of correlated transport. Large uncertainties in the measurement of such elements could also be partially responsible for the divergence of the elements in the factors. For example Ti and most of the INAA measurements are below detection limit or are missing values.

In the repeated running of ME, different local optima with different Q values were obtained. It was found that some factors switched between 2-way and 3-way in different local optima. For example, the iodine factor moved from a 3-way factor and MSA to 2-way factor in higher Q value (worse fitting) solutions. This phenomenon suggests that the periodicity of some sources is stronger than that of others, even though all factors show strength in the periodicity during the year as anticipated and shown as in Figs. 2 and 4.

The Cl/Na ratio in sea salt factor is 1.22 which is lower than their ratio in seawater, and there is higher SO_4^{2-} in this factor. This is quite reasonable when considering the replacement of Cl^- by acidic SO_4^{2-} during transport to Alert.

The MSA/SO_4^{2-} in the biogenic factor is 0.31 which is identical to the finding of Li et al. (1993) from isotope ratio analysis that this ratio is typically 0.31 for biogenic factor sulfur in the Arctic region. In a recent study of dimethylsulfide oxidation and the ratio of MSA to non sea-salt sulfate in the marine aerosol (Ayers et al. 1996), a latitude dependence of the aerosol MSA to non sea-salt SO_4^{2-} ratio and a strong temperature dependence of MSA decomposition were observed. Their results are also consistent with a ratio of 0.3.

The time variation of the soil factor shows a small peak in the spring and larger peaks in the later summer and early fall period. Previous studies pointed out that soil dust observed in the Arctic mainly comes from remote areas like distant Asian and African sources (Rahn et al., 1977; Pacyna et al., 1989). The peak in April/May may be associated in part with long-range transported desert dust from Asia raised by storms occurring in April and May; while the peak in September/October is probably caused by the onset of transport from areas sufficiently southern that there are areas of suspendable soil. Local areas can also be an origin of Arctic soil dust during blizzard weather conditions (Barrie et al., 1989).

In general, the year-to-year variations in the 3-way analysis are difficult to interpret. Since level of biogenic activity should be related to average temperature, the scores for this factor were plotted against the Northern Hemisphere temperature anomaly (Fig. 7) as obtained from Jones et al. (1997). Jones et al. (1986a–c), Jones (1988), Jones and Briffa (1992) and Briffa and Jones (1993) compiled these temperature results. A significant correlation between these quantities with a correlation coefficient of 0.72 was obtained. This result suggests that further examination of the concentration of MSA in remote locations may provide a good indicator for large-scale climate changes. Shaw (1983) had suggested the potential importance of particles produced from biogenic sources of reduced sulfur compounds. Charlson et al. (1987) pointed to ocean sources of dimethylsulfide leading to the formation of methane sulfonate and non sea-salt sulfate particles in the air. These biogenic sulfur

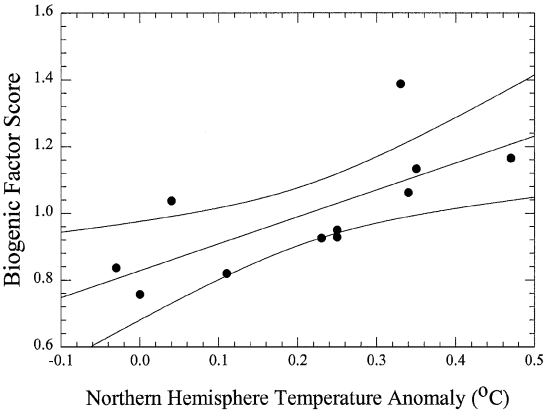

Fig. 7. Biogenic factor score against the Northern Hemisphere temperature anomalies for the time period from 1981 to 1991 relative to a reference period from 1950 to 1979 and corrected for El Nino.

sources should respond to changing temperature by producing additional reduced sulfur emissions. Bates and Quinn (1997) have very recently reported a possible increase in methyl disulfide in seawater from latitudes around the equator. Thus, these results may be the first indication of the interaction of climate with biogenic sulfur aerosol.

In the previous study (Xie et al., 1998), a similar but stronger correlation between the 3-way biogenic factor score and Northern Hemisphere temperature anomaly was obtained. Since *pure* 3-way modeling was used in that study, the higher correlation may come from the fact that more of the data variance was forced into the within-year time sequences.

6. Conclusion

ME has been used for the analysis of Arctic particle composition data from samples collected at Alert, Canada between 1980 and 1991 and a mixed 2-way/3-way model was assumed. The nature of the aerosol sources has been well explained by five 2-way and two 3-way factors. Possible sources with distinctive seasonal variations have been retrieved. The Arctic airborne particulate matter include particles derived from long-range transported anthropogenic pollutants, particles of long-range transported soil dust, sea salt aerosol, aerosols derived from acidic photochemical reactions of SO_2 to sulfuric acid, bromine and iodine release from the photolysis of organobromine and organoiodine which emitted from marine biological system and aerosol originated from biogenic activities at the surface of oceans. The resolved seasonal variations of the possible sources coincide with the earlier presented hypotheses.

Acknowledgements

The work at Clarkson University was supported by the National Science Foundation under grant OPP 9423252 and ATM 9523731. P. Paatero thanks the financial support from the Vilho, Yrjö and Kalle Väisälä Foundation.

References

Ayers, G.P., Cainey, J.M., Granek, H., Leck, C., 1996. Dimethylsulfide oxidation and the ratio of methanesulfonate to non sea-salt sulfate in the marine aerosol. Journal of Atmospheric Chemistry 25, 307–325.

Barrie, L.A., Hoff, R.M., 1984. The oxidation rate and residence time of sulfur dioxide in the Arctic atmosphere. Atmospheric Environment 18, 2711–2722.

Barrie, L.A., Hoff, R.M., 1985. Five years of air chemistry observations in the Canadian Arctic. Atmospheric Environment 19, 1995–2010.

Barrie, L.A., 1986. Arctic air pollution: an overview of current knowledge. Atmospheric Environment 20, 643–663.

Barrie, L.A., Bottenheim, J.W., Schnell, R.C., Crutzen, P.J., Rasmussen, R.J., 1988. Ozone destruction and photochemical reactions at polar sunrise in the lower Arctic troposphere. Nature 334, 138–141.

Barrie, L.A., DenHartog, G., Bottenheim, J.W., Landsberger, S., 1989. Anthropogenic aerosols and gases in the lower troposphere at Alert Canada in April 1986. Journal of Atmospheric Chemistry 9, 101–127.

Barrie, L.A., Barrie, M.J., 1990. Chemical components of lower tropospheric aerosols in the high Arctic: six years of observations. Atmospheric Chemistry 11, 211–226.

Bates, T.S., Quinn, P.K., 1997. Dimethylsulfide (DMS) in the equatorial Pacific Ocean (1982 to 1996): evidence of a climate feedback? Geophysical Research Letters 24, 861–864.

Bottenheim, J.W., Barrie, L.A., Altas, E., Heidt, L.E., Niki, H., Rasmussen, R.A., Shepson, P.B., 1990. Depletion of lower tropospheric ozone during Arctic spring: the polar sunrise experiment 1988. Journal of Geophysical Research 95, 18 555–18 568.

Bras, G.L., Platt, U., 1995. A possible mechanism for combined chlorine and bromine catalyzed destruction of tropospheric ozone in the arctic. Geophysical Research Letters 22, 599–602.

Briffa, K.R., Jones, P.D., 1993. Global surface air temperature variations over the twentieth century: Part 2, implications for large-scale high-frequency paleoclimatic studies. Holocene 3, 82–93.

Charlson, R.J., Lovelock, J.E., Andreae, M.O., Warren, S.G., 1987. Oceanic phytoplankton, atmospheric sulfur, cloud albedo and climate: a geophysiological feedback. Nature 326, 655–661.

Cheng, M.D., Hopke, P.K., Landsberger, S., Barrie, L.A., 1991. Distribution characteristics of trace elements and ionic species of aerosol collected at Canadian high Arctic. Atmospheric Environment 25 A, 2903–2909.

Cheng, M.D., Hopke, P.K., Barrie, L.A., Rippe, A., Olson, M., Landsberger, S., 1993. Qualitative determination of source regions of aerosol in Canadian high Arctic. Environmental Sciences and Technology 27, 2063–2071.

Ferek, R.J., Hobbs, P.V., Radke, L.F., Herring, J.A., Sturges, W.T., Cota, G.F., 1995. Dimethyl sulfide in the arctic atmosphere. Journal of Geophysical Research 100, 26 093–26 104.

Finlayson-Pitts, B., Livingston, F.E., Berko, H.N., 1990. Ozone destruction and bromine photochemistry at ground level in the Arctic spring. Nature 343, 622–625.

Heidam, N.Z., 1981. On the origin of the arctic aerosol– a statistical approach. Atmospheric Environment 15, 1421–1427.

Henry, R.C., 1987. Current factor analysis receptor models are ill-posed. Atmospheric Environment 21, 1815–1820.

Hopke, P.K., 1988. Target transformation factor analysis for aerosol source apportionment: a review and sensitivity study. Atmospheric Environment 22, 1777–1792.

Hopke, P.K., Receptor Modeling for Air Quality Management. Elsevier, Amsterdam, 1991.

Hopke, P.K., Barrie, L.A., Li, S.M., Cheng, M.D., Li, C., Xie, Y., 1995. Possible sources and preferred pathways for biogenic and non-sea-salt sulfur for the high Arctic. Journal of Geophysical Research 100, 16 595–16 603.

Jones, P.D., 1988. The influence of ENSO on global temperature. Climate Monitor 17, 80–89.

Jones, P.D., Briffa, K.R., 1992. Global surface air temperature variations over the twentieth century: Part 1, Spatial, temporal and seasonal details. Holocene 2, 105–179.

Jones, P.D., Wigley, T.M.L., Wright, P.B., 1986a. Global temperature variations between 1861 and 1984. Nature 322, 430–434.

Jones, P.D., Raper, S.C.B., Bradley, R.S., Diaz, H.F., Kelly, P.M., Wigley, T.M.L., 1986b. Northern Hemisphere surface air temperature variations: 1851–1984. Journal of Climate and Applied Metereology 25, 161–179.

Jones, P.D., Raper, S.C.B., Wigley, T.M.L., 1986c. Southern Hemisphere surface air temperature variations: 1851–1984. Journal of Climate and Applied Metereology 25, 1213–1230.

Jones, P.D., Wigley, T.M.L., Wright, P.B., 1997. Global and Hemisphere Annual Temperature Variations Between 1854 and 1991. Data Set No. NDP022R2 available from CDIAC, ORNL.

Levasseur, M., Gosselin, M., Michaud, S., 1994. A new source of dimethylsulfide (DMS) for the arctic atmosphere: ice diatoms. Marine Biology 121, 381–387.

Li, S.M., Barrie, L.A., 1993. Biogenic sulfur aerosol in the Arctic troposphere: 1. Contributions to total sulfate. Journal of Geophysical Research 98, 20 613–20 622.

Li, S.M., Barrie, L.A., Sirois, A., 1993. Biogenic sulfur aerosol in the Arctic troposphere: 2. Trends and seasonal variations. Journal of Geophysical Research 98, 20 623–20 631.

Nriagu, J.O., Coker, R.D., Barrie, L.A., 1991. Origin of sulfur in Canadian Arctic haze from isotopic measurements. Nature 349, 142–145.

Paatero, P., Tapper, U., 1993. Analysis of different modes of factor analysis at least squares fit problems. Chemom Intell Laboratory Systems 18, 183–194.

Paatero, P., Tapper, U., 1994. Positive matrix factorization: a non-negative factor model with optimal utilization of error estimates of data values. Environmetrics 5, 111–126.

Paatero, P., 1998. The multilinear Engine: a table-driven least squares program for solving all kinds of multilinear problems, including the n-way factor analytic PARAFAC model.

Journal of Computational and Graphical Statistics, January 1998, submitted.

Pacyna, J.M., Ottar, B., 1989. Origin of natural constituents in the Arctic aerosols. Atmospheric Environment 23, 809–815.

Rahn, K.A., Borys, R.D., and Shaw, G.E., 1977. The Asian source of Arctic haze bands. Nature 268, 713–715.

Sander, R., Vogt, R., Harris, G.W., Crutzen, P.J., 1997. Modeling the chemistry of ozone, halogen compounds and hydrocarbons in the Arctic troposphere during spring. Tellus 49B, 522–532.

Shaw, G.E., 1983. Bio-controlled thermostasis involving the sulfur cycle. Climate Change 5, 297–303.

Vogt, R., Crutzen, P.J., Sander, R., 1996. A mechanism for halogen release from sea-salt aerosol in the remote marine boundary layer. Nature 383, 327–330.

Xie, Y.L., Hopke, P.K., Paatero, P., Barrie, L.A., Li, S.M., 1998. Identification of source nature and seasonal variations of Arctic aerosol by positive matrix factorization. Journal of Atmospheric Science, in press.